Available online at www.sciencedirect.com
SCIENCE DIRECT®
Journal of Sound and Vibration 280 (2005) 863–882
JOURNAL OF SOUND AND VIBRATION
www.elsevier.com/locate/jsvi

Design of active controlled rotor-blade systems based on time-variant modal analysis

R.H. Christensen, I.F. Santos*

Building 358, Room 105, Department of Mechanical Engineering, Technical University of Denmark, DK-2800, Kgs. Lyngby, Denmark

Received 30 June 2003; accepted 18 December 2003
Available online 29 September 2004

Abstract

An active control system is developed to control blade as well as rotor vibrations in a coupled rotor–blade system where rotor lateral and blade flexible movements are coupled. In order to cope with the periodic time-varying dynamics of such systems, a periodic modal controller, based on time-variant modal analysis, is designed. The periodic time-varying equations of motion are transformed into a time-invariant modal form, which is used for designing the periodic controller. The modal decoupling of the equations of motion allows a system order reduction resulting in a simpler and more implementable controller addressing only specific vibration modes, which can cause problems. Moreover, the time-varying modal matrices, used for the modal decoupling, are also used for controllability and observability analyses in order to achieve optimal actuator and sensor placement in the system. The applicability of the controller design methodology is evaluated by a numerical example where a coupled periodic time-variant system built by a rigid rotor with four flexible blades is simulated. In the simulation model tip masses are added at the end of the blades with the aim of emphasizing the blade inertia effects and the time periodicity of the system. Rotor angular movements and the gyroscopic effect are neglected for simplicity, and the blades are modelled as flexible Bernoulli beams. Three different control schemes are designed using the described methodology. The results demonstrate that the designed controllers are capable to cope with the time periodicity of the system and suppress very efficiently only the vibration modes addressed.

*Corresponding author. Tel.: +45-45-25-62-69; fax: +45-45-88-15-51.
E-mail address: ifs@mek.dtu.dk (I.F. Santos).

0022-460X/$ - see front matter © 2004 Elsevier Ltd. All rights reserved.
doi:10.1016/j.jsv.2003.12.046

1. Introduction

Flexible rotating blades interacting with rotor lateral movement present some special dynamic peculiarities, which have to be clearly understood before active systems for vibration control can be properly designed and applied. Due to the centrifugal effects, the blade natural frequencies may significantly change depending on the rotor angular velocity, the so-called stiffening effect. Moreover, the variation of the blade position, when operating at constant angular velocities, leads to periodic variation of the inertia distribution in time, which can induce the appearance of parametric vibrations. Furthermore, the coupled rotor–blade mode shapes can occur extremely close to the flexural blade modes, hindering a precise identification of the different frequencies and introducing beating phenomena. The smaller the mass relationship between blades and rotor is, the closer are the coupled rotor–blade modes and the flexural blade modes [1].

Active control of vibrations in flexible structures has been extensively studied for several decades and applied to various types of systems [2–8] suppressing vibration among others in flexible bladed rotors and rotating beams. Nevertheless, most of the reported work only deals with linear time-invariant systems. For instance, active modal control of vibrations in a simple rotating cantilever beam is studied by Khulief [6]. Vibrations in rotating flexible blades using active piezoelectric actuation have been theoretically as well as experimentally investigated among others by Chen and Chopra [7] and Baz and Ro [8]. In these three reported works, the rotor lateral movement is neglected. When such a movement is also considered and the rotor operates at constant angular velocity, the system becomes periodic time-variant but current literature has dealt only with the problem of control design, with focus on blade vibration.

Several control methodologies, directed towards periodic systems, have been reported during the last two decades. For instance, an optimal periodic controller for helicopter vibration attenuation is designed by solving a periodic Ricatti equation [9] and a periodic $\mathscr{H}_\infty$ controller is designed in Ref. [10]. Lyapunov–Floquet transformation of the periodic system into a time-invariant form is used by many other authors. Hereby, linear time-invariant control techniques can be applied for the controller design. A technique for designing a pole placement state feedback controller by gain selection based on a modal transformation of the periodic system is described in Ref. [11]. In order to avoid real-time estimation of state variables in the periodic system, a design technique for an optimal output feedback controller with fixed gains based on a modal transformation of the periodic system is proposed in Ref. [12]. A method for designing periodic state feedback controllers using a Lyapunov–Floquet transformation method based on Chebyshev polynomials is reported in Ref. [13]. The efficiency of this methodology has been investigated in different types of systems, i.e. to control vibrations in a single parametrically excited rotating flexible beam [14] and to reduce vibrations in bladed discs by shaft-based actuation [15].

In the present paper, a periodic time-variant modal controller is designed, aiming to attenuate vibrations in a coupled rotor–blade system comprising four flexible rotating blades. While designing modal controllers, it is not always desirable to address and suppress all vibration modes, but only those which can cause significant damages to the machines. In this framework, the aim is to design a modal controller capable of addressing and suppressing specific selected vibration modes. Such a selection minimizes the order, complexity and energy consumption of the controller. By combining elements from the previously reported works, a state feedback controller

is designed similar to the method presented in Ref. [13], based on Chebyshev polynomials. However, in order to address the modal control concept, the system is transformed into a time-invariant form by the modal transformation technique for periodic systems, as presented in Ref. [12] and described in detail in Ref. [16]. The efficiency of applying this modal transformation for analysing and mathematically explaining parametric vibrations in coupled rotor–blade systems is described in [17] and for actively controlling them in Ref. [18]. Among the advantages of using the modal transformation for the controller design, one can mention that it allows a straightforward method for analysing the modal controllability and observability of the time-varying system. Moreover, it gives better physical interpretation and visualization of the time-varying mode shapes which are very useful, for example, for decisions regarding actuator and sensor placement. Therefore, when designing active controllers for such a special kind of mechanical systems, the periodic modal transformation becomes a very powerful tool.

2. Mathematical model

A mechanical model of the coupled rotor–blade system considered is shown in Fig. 1. The rotor shaft is assumed to be rigid and is mounted in a hub performing planar movement in the xy-plane. Four identical flexible blades with tip masses are radially attached to the rigid rotor and the motion of the blades is also assumed to be planar. Note that the movement of the rotor is assumed to be strictly restricted to the xy-plane, neglecting rotor angular movements and gyroscopic effects. This simplification allows a two-dimensional system to be used and also a system with a minimum number of degree of freedom. However, for practical use in real rotor-blade

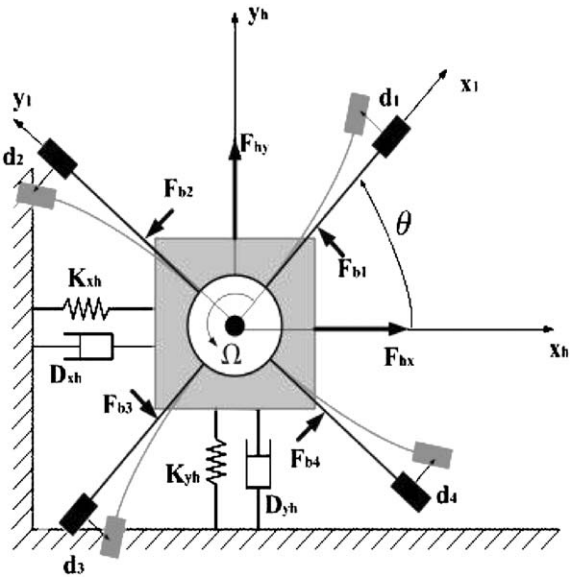

Fig. 1. Mechanical model of the coupled rotor–blade system: $x_h, y_h, d_1, d_2, d_3, d_4$ are the minimal coordinates for describing the rotor–blade system dynamics; $F_{h_x}, F_{h_y}, F_{b_1}, F_{b_2}, F_{b_3}, F_{b_4}$ are the active control forces and $K_{x_h}, K_{y_h}, D_{x_h}, D_{y_h}$ are the damping and stiffness of the hub foundation.

applications, the gyroscopic effects have to be considered. Nevertheless, neglecting the gyroscopic effect does not affect the main aim of the present theoretical work, i.e. an investigation and evaluation of a control design methodology for rotor–blade systems based on time-variant modal analysis.

In order to control vibrations in the system six actuation forces acting on the hub (F_{h_x} and F_{h_y}) and orthogonally on each of the blades (F_{b1}, F_{b2}, F_{b3} and F_{b4}) are applied to the system. Whether all six forces have to be applied to the system or only some of them, in order to be able to control the vibrations of the structure, will be analysed in Section 4.1.

The equations of motion for the rotor–blade system are derived using Lagrangian dynamics. Fig. 2 shows the coordinate systems and position vectors used to develop the model. Index I denotes the inertial reference frame attached to the non-moving foundation. The systems B_i and C_i denote auxiliary coordinate systems attached to the rotor, at the root of the ith blade, and to the ith blade tip mass, respectively.

The kinetic energy of the assembly is given by a sum of three contributions: (I) the rotor kinetic energy T_r; (II) the blade kinetic energy T_b and (III) the tip mass kinetic energy T_t. Axial elongation of the blades as well as the blade inertia are neglected in T_t. The total kinetic energy then is $T = T_r + T_b + T_t$, where

$$T_r = \tfrac{1}{2}J_h\dot{\theta}^2 + \tfrac{1}{2}m_h\, {}_I\dot{\mathbf{r}}_{oh}\cdot {}_I\dot{\mathbf{r}}_{oh}, \tag{1}$$

$$T_b = \sum_{i=1}^{4} \tfrac{1}{2}\rho_i \int_0^{L_i} {}_I\dot{\mathbf{r}}_{opi}(x_i)\cdot {}_I\dot{\mathbf{r}}_{opi}(x_i)\,\mathrm{d}x_i, \tag{2}$$

$$T_t = \sum_{i=1}^{4} \left[\tfrac{1}{2}m_{t_i}\dot{\mathbf{r}}_{ot_i}\cdot\dot{\mathbf{r}}_{ot_i} + \tfrac{1}{2}J_{t_i}\left(\dot{\theta} + \frac{\partial}{\partial x_i}\left(\dot{y}_i(L_i)\right)\right)^2 \right], \tag{3}$$

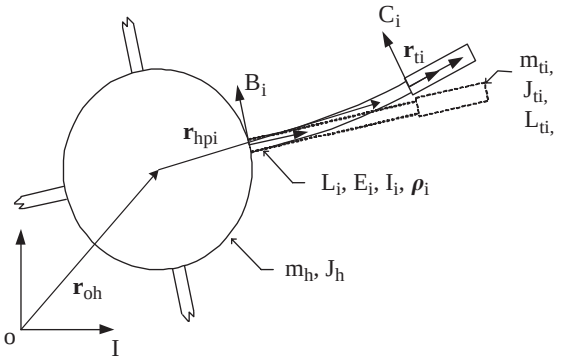

Fig. 2. The inertial and moving reference systems and position vectors used for derivation of the dynamic model. The geometrical and physical parameters L_i, ρ_i, E_i, I_i and $L_{t_i}, m_{t_i}, J_{t_i}$ relate to the ith blade and tip mass. The parameters m_h and J_h are the moment of inertia and the mass of the rotor and hub.

where $\dot{\mathbf{r}}$ denotes the time derivative of the displacement vector $\mathbf{r}$ defined in Fig. 2. The vector subscripts oh, op_i and ot_i indicate that the vectors $\mathbf{r}$ and $\dot{\mathbf{r}}$ describe the position and velocity of the rotor center point, a point located at the ith blade and the centre of gravity of the ith tip mass, relative to the point o. Index I denotes that the vectors are represented in terms of coordinates of the inertial reference frame.

The potential energy of the assembly consists also of three contributions: (I) the potential strain energy due to the elastic deformation of the blades V_e; (II) the gravity potential energy V_{gr} and (III) the geometric deformation potential energy V_g. The last term is required to take into account the centrifugal stiffening of the blades, which results in an increase of the blade natural frequencies as a function of the rotational speed [19]. Denoting the gravity vector ${}_I\mathbf{g}$ and the normal force acting on the beams by $N(x_i)$, the total potential energy is $V = V_e + V_{\mathrm{gr}} + V_g$, where

$$V_e = \sum_{i=1}^{4} \int_0^{L_i} \tfrac{1}{2} E_i I_i \left(\frac{\partial^2 y_i}{\partial x_i^2} \right)^2 \mathrm{d}x_i, \tag{4}$$

$$V_{gr} = m_h \, {}_I\mathbf{g} \cdot {}_I\mathbf{r}_{oh} + \sum_{i=1}^{4} \left[m_{t_i} \, {}_I\mathbf{g} \cdot {}_I\mathbf{r}_{ot_i} + \rho \int_0^{L_i} {}_I\mathbf{g} \cdot {}_I\mathbf{r}_{op_i}(x_i) \, \mathrm{d}x_i \right], \tag{5}$$

$$V_g = \sum_{i=1}^{4} \frac{1}{2} \int_0^{L_i} N(x_i) \left(\frac{\partial y_i}{\partial x_i} \right)^2 \mathrm{d}x_i. \tag{6}$$

The dynamic model is discretized by expressing the blade-bending deformation in terms of the n lowest mode shapes, that is

$$d_i(t, x_i) = \sum_{j=1}^{n} q_{ji}(t) \varphi_j(x_i) \quad \text{for } i = 1, 2, 3, 4 \text{ and } 0 \leqslant x_i \leqslant L_i, \tag{7}$$

where n is the number of modes, q_{ji} and $\varphi_j(x_i)$ are the modal coordinate and the mode shape function for the jth mode of the ith blade deflection, respectively. The general equations of motion for the coupled rotor–blade system are time-varying and functions of the rotor position θ, the rotational speed Ω and the acceleration $\dot{\Omega}$. The equations of motion are written as

$$\mathbf{M}(t)\ddot{\mathbf{z}}(t) + \mathbf{H}(t, \Omega)\dot{\mathbf{z}}(t) + \mathbf{K}(t, \Omega, \dot{\Omega})\mathbf{z}(t) = \mathbf{P}(t, \Omega, \dot{\Omega}) + \mathbf{Q}\mathbf{u}(t), \tag{8}$$

where $\mathbf{z}(t)_{(N\times 1)} = \{x_h, y_h, \mathbf{q}_1, \mathbf{q}_2, \mathbf{q}_3, \mathbf{q}_4\}^{\mathrm{T}}$ is a vector of generalized coordinates and $\mathbf{u}(t)_{(6\times 1)} = \{F_{h_x}, F_{h_y}, F_{b_1}, F_{b_2}, F_{b_3}, F_{b_4}\}^{\mathrm{T}}$ is a vector of control forces acting on the structure.

Rotating at constant speed the model becomes periodic time-variant with rotational frequency $\Omega = 2\pi/T$; that is,

$$\mathbf{M}(t) \equiv \mathbf{M}(t + T), \mathbf{H}(t) \equiv \mathbf{H}(t + T), \mathbf{K}(t) \equiv \mathbf{K}(t + T), \mathbf{P}(t) \equiv \mathbf{P}(t + T). \tag{9}$$

2.1. State space model for control

The equation of motion (8) is rewritten into a state-space form:

$$\dot{\mathbf{x}}(t) = \mathbf{A}(t)\mathbf{x}(t) + \mathbf{B}(t)\mathbf{u}(t) + \mathbf{F}(t), \tag{10}$$

with the vector of state variables $\mathbf{x}(t)^{\mathrm{T}}_{(2N\times 1)} = \{\mathbf{z}(t)^{\mathrm{T}}\dot{\mathbf{z}}(t)^{\mathrm{T}}\}$ and the system matrices

$$\mathbf{A}(t)_{(2N\times 2N)} = \begin{bmatrix} 0 & I \\ -\mathbf{M}(t)^{-1}\mathbf{K}(t) & -\mathbf{M}(t)^{-1}\mathbf{H}(t) \end{bmatrix}, \tag{11}$$

$$\mathbf{B}(t)_{(2N\times 6)} = \begin{bmatrix} \mathbf{0} \\ \mathbf{M}(t)^{-1}\mathbf{Q} \end{bmatrix}, \quad \mathbf{F}(t)_{(2N\times 1)} = \begin{Bmatrix} \mathbf{0} \\ \mathbf{M}(t)^{-1}\mathbf{P}(t) \end{Bmatrix}. \tag{12}$$

The output equation is given by $\mathbf{y}(t) = \mathbf{C}\mathbf{x}(t),$, where $\mathbf{C}$ is defined in such a way that the outputs are the lateral position of the hub and the tip point deflections of the blades $\mathbf{y}(t)_{(6\times 1)} = \{x_h, y_h, d_1, d_2, d_3, d_4\}^{\mathrm{T}}$.

2.2. Modal transformed model

By using a periodic modal transformation Eq. (10) is transformed into a system of independent equations of motion, where each equation represents one vibration mode. This modal formulation is obtained by introducing a vector of modal state variables $\xi(t)$ defined by $\mathbf{x}(t) = \mathbf{R}(t)\xi(t)$ where $\mathbf{R}(t)$ is the right modal matrix. Introducing this new state vector, the system is rewritten to the form

$$\dot{\xi}(t) = \mathscr{A}\xi(\mathrm{t}) + \mathscr{B}(t)\mathbf{u}(t) + \mathscr{F}(t), \quad \mathbf{y}(t) = \mathscr{C}(t)\xi(t), \tag{13}$$

where $\mathscr{A} = [\mathbf{L}^{\mathrm{T}}(t)\mathbf{A}(t)\mathbf{R}(t) - \mathbf{L}^{\mathrm{T}}(t)\dot{\mathbf{R}}(t)]$ is a constant diagonal matrix containing the eigenvalues of $\mathbf{A}(t)$ along the diagonal, $\mathscr{B}(t) = \mathbf{L}^{\mathrm{T}}(t)\mathbf{B}(t)$ is the periodic oscillatory modal control matrix, $\mathscr{F}(t) = \mathbf{L}^{\mathrm{T}}(t)\mathbf{F}(t)$ is the periodic oscillatory vector of modal forces and $\mathscr{C}(t) = \mathbf{C}\mathbf{R}(t)$ is the periodic modal output matrix.

The right $\mathbf{R}(t)$ and left modal matrix $\mathbf{L}^{\mathrm{T}}(t)$ used for the transformation are periodic time-variant and they are determined by solving the time-variant eigenvalue problem $\dot{\mathbf{r}}(t) + [\lambda\mathbf{I} - \mathbf{A}(t)]\,\mathbf{r}(t) = 0$ using Hill's method of infinite determinants [16, 17,20]. The efficiency of applying this modal transformation technique for analysing coupled rotor–blade systems and for mathematically explaining the presence of parametric vibrations of such systems is carefully investigated in Ref. [17]. Using this methodology the modal matrices are given by

$$\mathbf{R}(t) = \mathbf{R}(t+T) = \sum_{j=-n}^{n} \mathbf{R}_j e^{ij\Omega t}, \quad \mathbf{R}(t)\mathbf{L}^{\mathrm{T}}(t) = \mathbf{I}. \tag{14}$$

The Fourier coefficients $\mathbf{R}_j$ represent basis and parametric vibration mode components of the system. The basis modes, corresponding to the eigenvalues λ, are given by $\mathbf{R}_0$ and parametric vibration modes are given by $\mathbf{R}_j$, corresponding to the eigenvalues $\lambda + \mathrm{ij}\Omega$. That means the modal coordinates $\xi(t)$ of the transformed system address both type of modes, i.e. the basis modes and the associated parametric modes. Therefore, reducing the vibration amplitude of hub and blades

using the representation in the modal state coordinates $\boldsymbol{\xi}(t)$ implies that the basis as well as the parametric modes will be reduced.

2.3. Reduced order model

In order to reduce the order of the controller and state observer, the system is reorganized into a subset of controlled modes and a set of residual modes, denoted by the indices c and r, respectively. The controller is designed to suppress only specific vibration modes, thus considering the remaining insignificant, non-controllable or non-observable modes as residual modes. The reduced modal system is written as

$$\begin{Bmatrix} \dot{\boldsymbol{\xi}}_c(t) \\ \dot{\boldsymbol{\xi}}_r(t) \end{Bmatrix} = \begin{bmatrix} \mathscr{A}_c & \mathbf{0} \\ \mathbf{0} & \mathscr{A}_r \end{bmatrix} \begin{Bmatrix} \dot{\boldsymbol{\xi}}_c(t) \\ \dot{\boldsymbol{\xi}}_r(t) \end{Bmatrix} + \begin{bmatrix} \mathscr{B}_c(t) \\ \mathscr{B}_r(t) \end{bmatrix} \mathbf{u}(t) + \begin{Bmatrix} \mathscr{F}_c(t) \\ \mathscr{F}_r(t) \end{Bmatrix}. \tag{15}$$

Such an order reduction implies that precautions have to be taken in order to avoid control and observation spill-over problems. Moreover, for practical implementation, modelling errors and non-modelled dynamics will also result in such problems. In this entirely numerical study, control and observation spill-over will not cause significant problems and will therefore not be studied in details. However, spill-over is an important topic when designing vibration controllers and has to be considered for practical implementation. For such implementation, it might be necessary to take precautions such as implementing band-pass filters to prevent excitation of non-controlled modes and to prevent the presence of residual modes in the measured variables. Residual modes mean all modes higher than those considered in the reduced mathematical model.

2.4. Model of non-complex coefficients

Due to the complex eigenvalues, and eigenvectors the modal model contains complex coefficients. Therefore, for controller design reasons the complex model is rewritten into a real form by separating the real and imaginary parts

$$\dot{\bar{\boldsymbol{\xi}}}(t) = \bar{\mathscr{A}}\bar{\boldsymbol{\xi}}(t) + \bar{\mathscr{B}}(t)\mathbf{u}(t) + \bar{\mathscr{F}}(t), \quad \bar{\mathbf{y}}(t) = \bar{\mathscr{C}}(t)\bar{\boldsymbol{\xi}}(t), \tag{16}$$

where the new state vector and the matrices $\bar{\mathscr{A}}, \bar{\mathscr{B}}(t)$ and $\bar{\mathscr{C}}(t)$ are given by

$$\bar{\boldsymbol{\xi}}(t)_{(2N_c\times 1)} = \left\{\Re(\xi_{c,1}), \Im(\xi_{c,1}), \Re(\xi_{c,2}), \Im(\xi_{c,2}), \ldots, \Re(\xi_{c,N_c}), \Im(\xi_{c,N_c})\right\}^{\mathrm{T}}, \tag{17}$$

$$\bar{\mathscr{A}}_{(2N_c\times 2N_c)} = \begin{bmatrix} \ddots & & \mathbf{0} \\ & \bar{\mathscr{A}}_{ii} & \\ \mathbf{0} & & \ddots \end{bmatrix} \quad \text{where} \quad \bar{\mathscr{A}}_{ii} = \begin{bmatrix} \Re(\lambda_i) & -\Im(\lambda_i) \\ \Im(\lambda_i) & \Re(\lambda_i) \end{bmatrix}, \tag{18}$$

$$\bar{\mathscr{B}}(t)_{(2N_c\times 6)} = \left[\Re(\mathscr{B}_{c,1}), \Im(\mathscr{B}_{c,1}) \ldots \Re(\mathscr{B}_{c,N_c}), \Im(\mathscr{B}_{c,N_c})\right]^{\mathrm{T}}, \tag{19}$$

$$\bar{\mathscr{C}}(t)_{(6\times 2N_c)} = \left[\Re(\mathscr{C}_{c,1}), -\Im(\mathscr{C}_{c,1}) \ldots \Re(\mathscr{C}_{c,N_c}), -\Im(\mathscr{C}_{c,N_c})\right]. \tag{20}$$

N_c denotes the number of controlled modes.

3. Active controller design

3.1. Modal controllability and observability

The controllability and observability depend on the number and location of actuators and sensors. Therefore, in order to determine the minimum number and optimal placement of actuators and sensors in the system, the modal controllability and observability are analysed.

Generally, the system is modal controllable if no row of the modal control matrix consists only of zeros and all modes are observable if no column of the modal output matrix consists only of zeros. However, these are poor measures of the modal controllability and observability. Better measures are provided in [21], for time-invariant systems, which provides quantitative indices of how controllable and observable a specific mode is from all inputs and outputs. For the time-varying case, such measures are given by

$$\mathrm{MC}_i(t) = \mathrm{norm}\left(\frac{\mathbf{l}_i^{\mathrm{T}}(t)\cdot\mathbf{B}(t)}{||\mathbf{l}_i^{\mathrm{T}}(t)||}\right), \quad \mathrm{MO}_i(t) = \mathrm{norm}\left(\frac{\mathbf{C}\cdot\mathbf{r}_i(t)}{||\mathbf{r}_i(t)||}\right), \tag{21}$$

where $\mathbf{r}_i(t)$ and $\mathbf{l}_i^{\mathrm{T}}$ are the ith right and left eigenvectors, respectively.

As an alternative to this methodology of studying the controllability and observability by calculating quantitative measures, the controllability and observability can be also studied by observing the mode shapes. The larger the amplitude of the mode shape is at the location of actuators or sensors, the more controllable or observable is the system.

3.2. Periodic controller design

Using the periodic oscillatory modal model, Eq. (16), a time-periodic controller for the original periodic system, Eq. (10), is designed using the traditional time-invariant control technique. A time-periodic state feedback controller is designed by a methodology similar to the method used in Ref. [13], although, it is based on the modal transformed model. The time-variant state feedback control law is defined by

$$\mathbf{u}(t) = \bar{\mathscr{G}}(t)\bar{\boldsymbol{\xi}}(t). \tag{22}$$

Substituting $\bar{\mathscr{B}}(t)$ with a constant matrix $\bar{\mathscr{B}}_0$, i.e. given by the value of $\bar{\mathscr{B}}(t)$ at a specific instant of time, and neglecting the modal force vector, the modal model, Eq. (16), is given by

$$\dot{\bar{\boldsymbol{\xi}}}(t) = \bar{\mathscr{A}}\bar{\boldsymbol{\xi}}(t) + \bar{\mathscr{B}}_0\mathbf{u}_0(t). \tag{23}$$

If the system is non-controllable or only weakly controllable at specific instants of time, the matrix $\bar{\mathscr{B}}_0$ has to be carefully chosen in order to avoid problems. For this time-invariant system, Eq. (23), a control law is defined by

$$\mathbf{u}_0(t) = \bar{\mathscr{G}}_0\bar{\boldsymbol{\xi}}(t), \tag{24}$$

where $\bar{\mathscr{G}}_0$ is a constant gain controller designed using traditional linear time-invariant control technique, for instance by LQ design.

By 'equalizing' the periodic oscillatory system, Eq. (16), and the rewritten time-invariant system, Eq. (23), the constant gain controller is transformed into a periodic form. The periodic controller gain matrix then is

$$\bar{\mathscr{G}}(t) = \left[\bar{\mathscr{B}}^{\mathrm{T}}(t)\bar{\mathscr{B}}(t)\right]^{-1}\bar{\mathscr{B}}^{\mathrm{T}}(t)\bar{\mathscr{B}}_0\bar{\mathscr{G}}_0. \tag{25}$$

3.3. Periodic state observer design

All state variables are not directly measureable. Therefore, a deterministic time-periodic observer is designed to estimate the state variables. The periodic observer equation is given by

$$\dot{\hat{\bar{\xi}}}(t) = \bar{\mathscr{A}}\hat{\bar{\xi}}(t) + \bar{\mathscr{B}}(t)\mathbf{u}(t) + \bar{\mathscr{F}}(t) + \bar{\mathscr{G}}_{\mathrm{obs}}(t)\left(\mathbf{y}(t) - \bar{\mathscr{C}}(t)\hat{\bar{\xi}}(t)\right), \tag{26}$$

where $\hat{\bar{\xi}}(t)$ denotes the estimated state variables, $\mathbf{y}(t)$ the measured variables and $\bar{\mathscr{G}}_{\mathrm{obs}}(t)$ the observer gain matrix.

It is well known that the observer gain matrix for a time-invariant system can be determined by designing a controller for the dual system. Using this property, the periodic time-varying observer gain matrix can be designed by a procedure similar to the controller design procedure. The dual system is given by

$$\dot{\bar{\xi}}_d(t) = \bar{\mathscr{A}}^{\mathrm{T}}\bar{\xi}_d(t) + \bar{\mathscr{C}}^{\mathrm{T}}(t)\mathbf{u}_d(t). \tag{27}$$

Again introducing a constant matrix $\bar{\mathscr{C}}_0$, so that the dual system is time-invariant and controllable, a constant gain controller $\bar{\mathscr{G}}_{e,0}$ is designed for the dual system. The periodic observer gain matrix is then given by

$$\bar{\mathscr{G}}^{\mathrm{T}}_{\mathrm{obs}}(t) = \left[\bar{\mathscr{C}}(t)\bar{\mathscr{C}}^{\mathrm{T}}(t)\right]^{-1}\bar{\mathscr{C}}(t)\mathscr{C}_0^{\mathrm{T}}\bar{\mathscr{G}}_{e,0}. \tag{28}$$

4. Numerical results

The performance of the designed control methodology is examined by numerical simulations. The parameters of the rotor–blade system used for this numerical analysis are given in Tables 1 and 2.

4.1. Sensor and actuator placement

Placement of actuators and sensors in an active controlled bladed rotor system is very important from a machinery design point of view. The costs and difficulties related to the implementation depend very strongly on the type, quantity and placement of the actuators and sensors implemented in the system. For example, actuators and sensors can be located on the blades monitoring and acting directly on them, or they can be located on the rotor, monitoring

Table 1
Rotor properties

Rotor/Hub	
Mass	$m_{h_x} = 2.0\ \text{kg};\ m_{h_y} = 2.0\ \text{kg}$
Stiffness	$K_{x_h} = 6 \times 10^3\ \text{N/m};\ K_{y_h} = 8 \times 10^3\ \text{N/m}$
Damping	$D_{x_h} = 10^{-6}\ \text{N s/m};\ D_{y_h} = 10^{-6}\ \text{N s/m}$
Inertia	$J_h = 10^{-2}\ \text{kg m}^2$
Excentricity	$\varepsilon = 10^{-3}\ \text{m}; k = 0\ \text{rad}$
Diameter	$r = 0.04\ \text{m}$
Rotor mass	$m_r = 0.5\ \text{kg}$

Table 2
Blade properties

Blades and Tip masses	
Length	$L_i = 80 \times 10^{-3}\ \text{m}$
Width	$b_i = 25 \times 10^{-3}\ \text{m}$
Thickness	$h_i = 10^{-3}\ \text{m}$
Density	$\rho = 7800\ \text{kg/m}^3$
Elasticity	$E_i = 2.0 \times 10^{11}\ \text{N/m}^2$
Locations	$\alpha_i = (i-1)\pi/2\ \text{rad};\ i = 1, 2, 3, 4$
Tip mass	$m_{t_i} = 0.100\ \text{kg}$
Tip inertia	$J_{t_i} = 3.35 \times 10^{-5}\ \text{kg m}^2$
Tip mass length	$L_{t_i} = 30 \times 10^{-3}\ \text{m}$

and acting directly on the rotor. Placing the actuators and sensors in the rotating blades introduces several difficulties to be overcome compared to the alternative placement. Measurement and control signals have to be transmitted between the rotating frame and the control unit using slip rings or telemetric transmission techniques. This increases the machinery complexity and development costs significantly. Moreover, when built into the rotating blades, actuators and sensors have to be resistant to harsh working conditions, such as fatigue failure and severe pressure, flow or temperature conditions.

Actuators and sensors can be implemented into active controlled rotor–blade systems using various types of actuation and sensing techniques. Such implementation relies very much on the specific rotor–blade system. In practice, blade actuation can be applied to rotor-blade systems using variable geometry actuators [22] or piezo-electric actuators embedded into the blades [8]. Blade vibrations can be monitored using measurement techniques such as strain guages or piezo-electric elements attached directly on the blades. For some large structures, the use of acceleration measurements will also be possible. Alternatively, in order to avoid the transmission of measurement signals from the rotating system to the inertial frame, sensors fixed in the inertial frame can also be used in some practical applications [23]. A review of the current state of the art

regarding rotor–blade vibration monitoring methods is provided in Ref. [24]. Monitoring and controlling vibrations by placing actuators and sensors directly onto the rotor are much less problematic. Many different types of active bearings have been developed, for instance, electromagnetic bearings [25,26], piezo-electric actuated bearings [27], active lubricated bearings [28] or hydraulic actuated bearings [29,30], and can be used to achieve this goal.

The practical difficulties and increasing costs related to the implementation of actuators and sensors in the rotating blades compared to the implementation of active controlled bearings motivate this investigation: Answers to a number of questions are sought. These are: are actuators and sensors fixed to the blades necessary? are the placement of such actuators and sensors in the blades inevitable in order to monitor and control vibrations in bladed rotor systems? can the rotor as well as blade vibrations be controlled solely by means of rotor/hub-based actuation? To investigate this, the controllability and observability of the rotor–blade system are analysed in order to determine where to place sensors and actuators capable of monitoring and controlling the rotor–blade vibrations.

4.1.1. Time-variant modal analysis in the rotor–blade system

Figs. 3–5 show the basis mode shape components given by the Fourier coefficients $\mathbf{R}_0$ and the parametric mode shape components of order $+1$ and -1 given by $\mathbf{R}_{+1}$ and $\mathbf{R}_{-1}$. Parametric modes of higher order are not presented because these are very small and insignificant in the system response. The number in the lower left corner of the plots in the figures denotes a normalization factor. Generally speaking, the lower the normalization factor of a mode is, the more significant will be the contribution of such a mode to the dynamic response of the system. The factor "inf" means that the normalization factor is almost infinite, consequently, these modes are not normalized and will not significantly influence the response of the system.

For a correct understanding of the physical meaning of M1…M10, P1…P10 and R1…R10, these shapes have to be simultaneously analysed. For example, the first mode shape of the rotor–blade system is built by M1, P1 and R2. M1 is associated to the stationary or non-rotating part of the mode and contributes strongly to the system response, factor 1.0. P1 is associated to

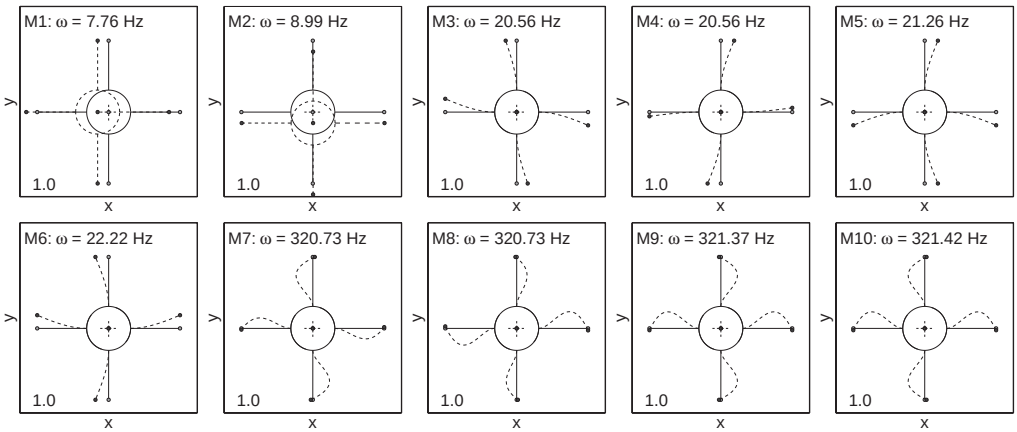

Fig. 3. Basis mode shapes for the coupled rotor–blade system given by $\mathbf{R}_0$.

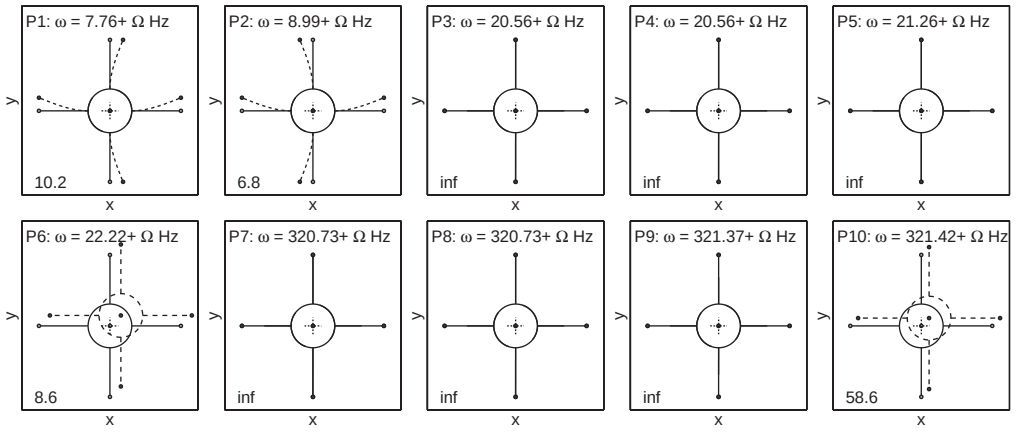

Fig. 4. Parametric mode shapes of order $+1$ for the coupled rotor–blade system given by $\mathbf{R}_{+1}$.

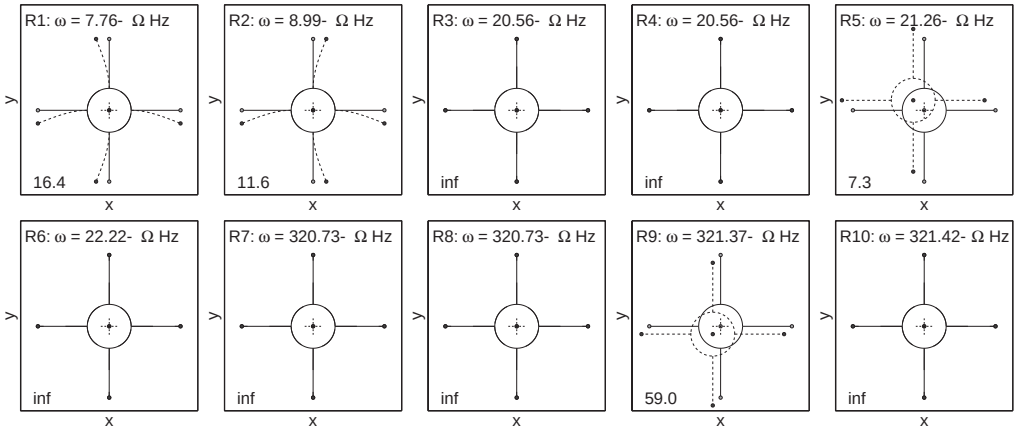

Fig. 5. Parametric mode shapes of order -1 for the coupled rotor-blade system given by $\mathbf{R}_{-1}$.

the forward rotating part of the mode shape, factor 1/10.2. The backward rotating part of the mode, named R1, does not contribute much to the mode, once the factor is 1/16.4. By checking the mode shapes, it is easy to see the necessity of mounting actuators which act on the hub as well as on the blades in order to control all mode shapes. Naturally, the hub-based actuators are necessary to control the rigid body motion of the rotor. Theoretically, modes 1, 2, 5, 6, 9 and 10 can be controlled by hub actuation only, due to the amplitude of rotor motion in the stationary parts M1 and M2 of modes 1 and 2; in the backward rotating part R5 of mode 5; in the forward rotating part P6 of mode 6; in the backward rotating part R9 of mode 9 and in the forward rotating part P10 of mode 10. This implies that theoretically the mode components M5, M6, M9, M10, P1, P2, R1 and R2 can also be controlled by hub actuation. However, the remaining significant components M3, M4, M7 and M8 of the 3rd, 4th, 7th and 8th modes cannot be

controlled by the hub-based actuators because these modes are decoupled from the hub movement. Consequently, actuators have to act on the blades to control these modes. Similarly, it is necessary to mount sensors on both the hub and on the blades to estimate all state variables.

4.1.2. Quantitative measures of controllability and observability

An indication of where to locate actuators and sensors was obtained from the mode shape analysis. In order to make a definitive decision on where to locate the actuators and sensors, the controllability and observability of four different actuator and sensor configurations, shown in Fig. 6, are analysed. The actuators can be mounted so that they act on the rotor shaft, configuration (a), act directly on the blades, configurations (b) and (c), or act on both rotor and blades, configuration (d). Sensors are assumed to be mounted at the same positions to measure the position of the hub or the deflection of the blades.

In general, the controllability and observability indices $MC_i(t)$ and $MO_i(t)$ are time-variant. However, for the actual coupled rotor–blade system, the indices become almost constant, oscillating only very slightly due to scaling difference among the constant and the periodic varying components of the mode shapes. Table 3 shows the minimum values of the controllability indices for the first 10 modes, using four different configurations related to actuator placement. Such indices are normalized, allowing a direct comparison between the four configurations, and the minimum values are obtained inside a time interval of one period. The higher the controllability index, the more controllable is the mode. For comparison purpose the indices are all normalized by referring to the most controllable mode which is mode 6 for configuration (b). The results show

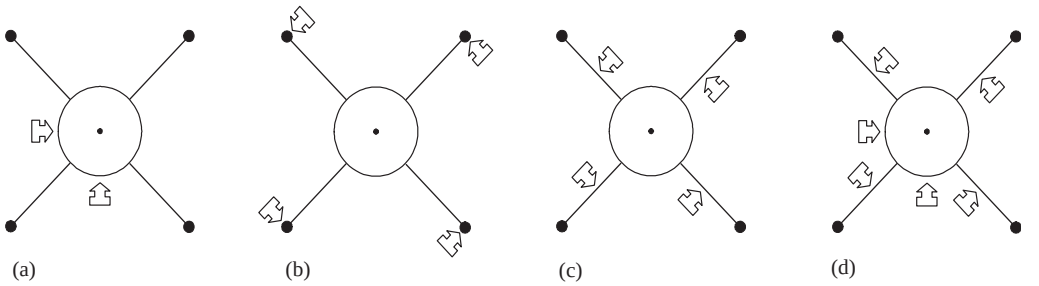

Fig. 6. The four actuator and sensor configurations analysed to obtain optimal actuator and sensor placement.

Table 3
Measure of controllability of each mode for the four system configurations — MC index.

Actuator configuration	Mode no.									
	1	2	3	4	5	6	7	8	9	10
(a)	0.13	0.12	0.00	0.00	0.08	0.07	0.00	0.00	0.00	0.00
(b)	0.04	0.02	0.94	0.94	0.91	1.00	0.04	0.04	0.04	0.04
(c)	0.01	0.01	0.24	0.24	0.23	0.25	0.25	0.25	0.25	0.25
(d)	0.13	0.12	0.24	0.24	0.24	0.26	0.25	0.25	0.25	0.25

Table 4
Measure of observability of each mode for the four system configurations — MO index.

Sensor configuration	Mode no.									
	1	2	3	4	5	6	7	8	9	10
(a)	1.00	0.82	0.00	0.00	0.04	0.03	0.00	0.00	0.00	0.00
(b)	0.28	0.33	0.48	0.48	0.46	0.44	0.00	0.00	0.00	0.00
(c)	0.07	0.09	0.12	0.12	0.12	0.11	0.03	0.03	0.03	0.03
(d)	1.00	0.83	0.12	0.12	0.12	0.11	0.03	0.03	0.03	0.03

that application of only hub-based actuation (a) implies that only modes 1, 2, 5 and 6 can be controlled. For configuration (b) where actuators act at the tip of the blades, close to the node of the blades' 2nd mode shape, the indices show that only the modes related to the first mode of the blades (modes 3–6 in Table 3) can be controlled. For configuration (c), where the actuators act on the middle of the blades, all blade modes 3–10 can be controlled. Finally, when actuators act on both the hub and the blades, configuration (d), all 10 modes of the system can be controlled. Consequently, in the numerical example both hub and blade actuators are applied to the system. The normalized result of the equivalent observability analysis, (Table 4), provides similar results. Simultaneous sensing of hub and blade movements is necessary in order to estimate all state variables.

By comparison of the result of this controllability and observability analysis with the observations of the mode shapes in the Figs. 3–5, the validity of the controllability and observability indices in Table 3 and 4 is easily verified.

4.2. Controller design

Using the controller design procedure described, active controllers are designed to control the dynamics of specific selected vibration modes, thus treating the remaining modes as residual modes. The controller gains are determined by the optimal quadratic control technique (LQR) minimizing the cost function:

$$J = \int \left(\bar{\boldsymbol{\xi}}^{\mathrm{T}} \mathbf{Q}_{\xi} \bar{\boldsymbol{\xi}} + \mathbf{u}^{\mathrm{T}} \mathbf{Q}_{u} \mathbf{u} \right) \mathrm{d}t, \tag{29}$$

where the elements of the state variable weighting matrix $\mathbf{Q}_{\xi}$ are shown in Table 5 and the control signal-weighting matrix is given by $\mathbf{Q}_{u} = 10^{-2} \cdot \mathbf{I}_{6}$. Three different controller configurations are designed and examined by numerical simulations. The first controller is designed to control only the first mode, the second controller to reduce all modes primarily related to the first bending mode of the blades (modes 3–6) and the third controller to reduce the first six modes of the rotor–blade system. Modes 7–10 are considered as residual modes in all three controllers and for the numerical evaluation of the performance of the designed controllers a model of 10 modes is used.

Table 5
Diagonal elements of the controller design weighting matrix $\mathbf{Q}_{\xi}$

Control scheme	Modes basis frequency [Hz]									
	ω_1	ω_2	ω_3	ω_4	ω_5	ω_6	ω_7	ω_8	ω_9	ω_{10}
	7.76	8.99	20.56	20.56	21.26	22.22	320.73	320.73	321.37	321.42
$\bar{\mathcal{G}}_1$:	10^4	—	—	—	—	—	—	—	—	
$\bar{\mathcal{G}}_2$:	—	—	10^2	10^2	10^2	10^2	—	—		—
$\bar{\mathcal{G}}_3$:	10^4	10^4	10^2	10^2	10^2	10^2	—	—		—

4.2.1. Time response analysis

Fig. 7 shows the transient response of the first six modal state variables for the non-controlled system and for the system controlled using the three designed controllers. The rotor–blade system rotates at the constant speed $\Omega = 5$ Hz and the initial conditions of the position state variables are $\mathbf{z}(0) = \{-5; -5; 5; 0; 5; 0; -5; 0; 5; 0\}^{\mathrm{T}} \cdot 10^{-3}$ m and zero velocities $\dot{\mathbf{z}}(0) = \mathbf{0}$ m/s. The responses in Fig. 7 are difficult to discriminate, but the plots show the expected responses. The control scheme 1 reduces only the first mode significantly, while the other modal coordinates are almost unaffected. Spill-over effects are observed in the modal state variables by the excitation of the higher modes 7–10. These modes are excited in the numerical simulation only because the actuators are considered to be ideal actuators acting instantaneously with no time delay and because the sampling frequency ($T_s = 0.001$ s) is higher than the excited frequencies. Control scheme 2 reduces only modes 3–6 while scheme 3 suppresses all the first six modes.

Figs. 8–10 show the transient responses of the physical variables x_h, y_h and d_2 of the non-controlled and the controlled system for the three designed controllers. Mode 1 mostly contributes to the hub movement in the x-direction, and therefore control scheme 1 primarily reduces this movement. However, due to the vibration coupling between the rigid rotor and the blades, the first mode of the system is not purely related to the hub movement in the x-direction, but also slightly related to the blade motions, according to the mode shapes in Figs. 3–5. Therefore, the blade deflection is also very slightly affected when controlling the first mode. For control scheme 2 the figures show that only the blade motions primarily related to modes 3–6 are suppressed, while the hub movements are only slightly affected due to the coupling. For control scheme 3, the transient responses show that x_h, y_h and d_2 are all very efficiently reduced.

4.2.2. Frequency response analysis

The frequency response for the system subjected to an impulse excitation is given by [31]

$$\mathbf{X}(\omega) = \sum_{v=-n}^{n} \sum_{u=-n}^{n} \mathbf{R}_v \left[\cdot \quad \frac{1}{j(\omega - v\Omega) - \lambda_{i,0}} \quad \cdot \right] \mathbf{L}_u^{\mathrm{T}} \mathbf{f}_0, \tag{30}$$

where $\mathbf{f}_0$ is a vector of frequency spectra of the exciting forces, which is constant for an impulse excitation and $\lambda_{i,0}$ denotes the basis eigenvalue for the ith mode. The matrices $\mathbf{R}_v$ and $\mathbf{L}_u^{\mathrm{T}}$ now represent Fourier expansion coefficients of the modal matrices for the closed form of the controlled system. Neglecting the observer dynamics and transforming the controller into physical

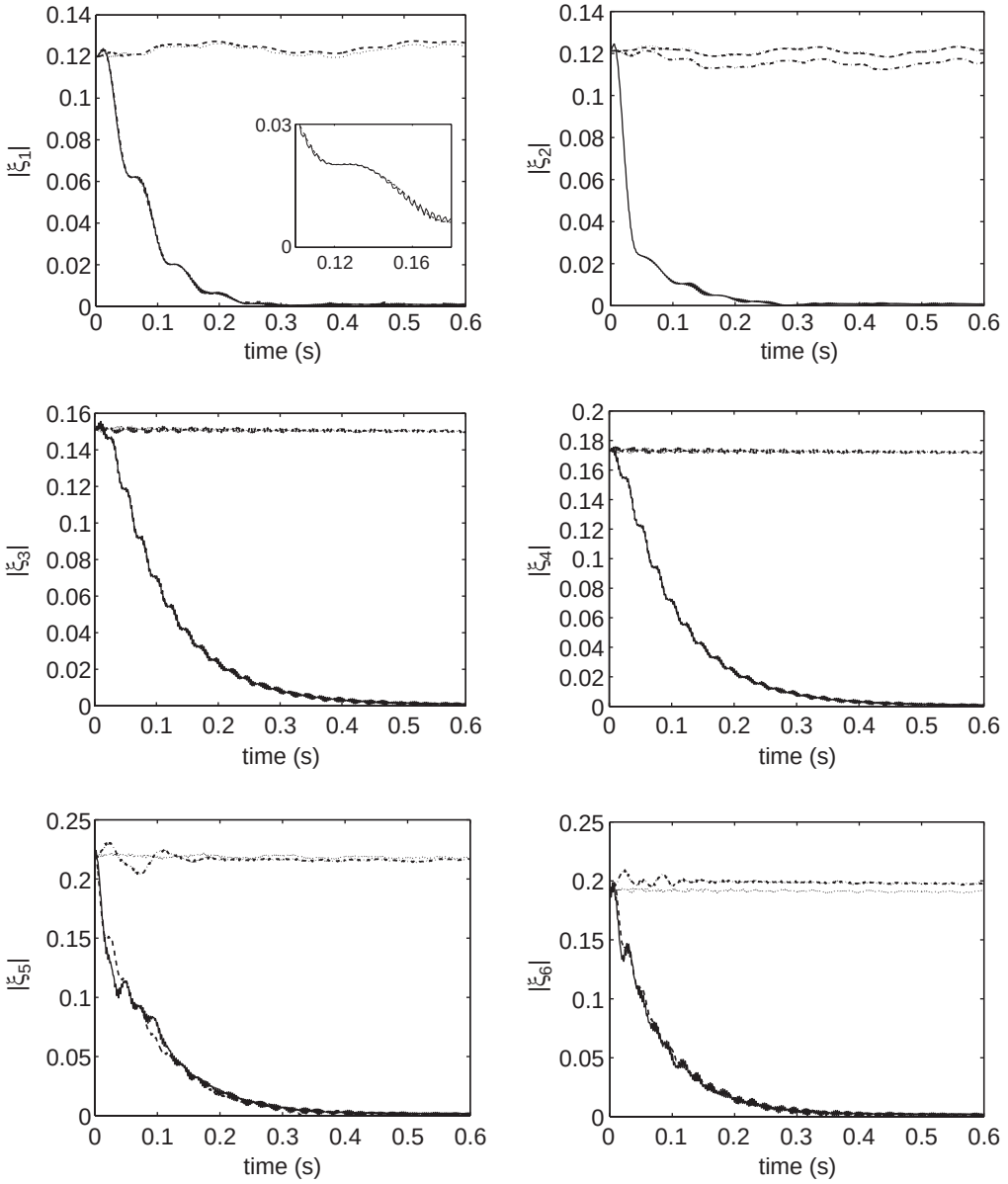

Fig. 7. The first six modal state variables of the controlled and non-controlled system. The non-controlled response ($\cdots$), control by scheme 1 ($-\cdot-$), by scheme 2 ($--$) and by scheme 3 (—).

variables $\mathbf{G}(t)$, the closed form is given by

$$\dot{\mathbf{x}}(t) = [\mathbf{A}(t) + \mathbf{B}(t)\mathbf{G}(t)]\mathbf{x}(t) + \mathbf{F}(t). \tag{31}$$

Fig. 11 shows the frequency responses of the lateral movement of the rotor and the deflection of blade 2 for the controlled as well as the non-controlled system, when the system is subjected to an impulse excitation acting on the rotor and on blade 2, respectively. Again, the lines of the spectra are difficult

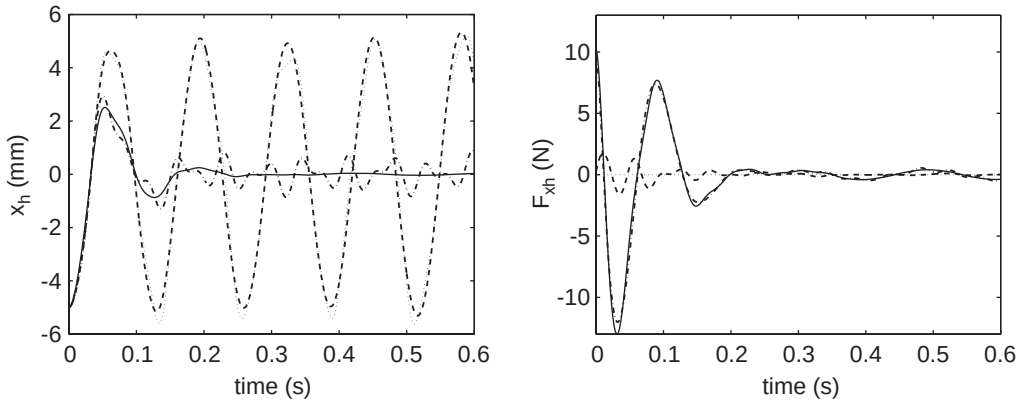

Fig. 8. Hub movement in the x-direction and the control force applied using the three designed control schemes. The non-controlled response ($\cdots$), control by scheme 1 ($-\cdot-$), by scheme 2 ($--$) and by scheme 3 (—).

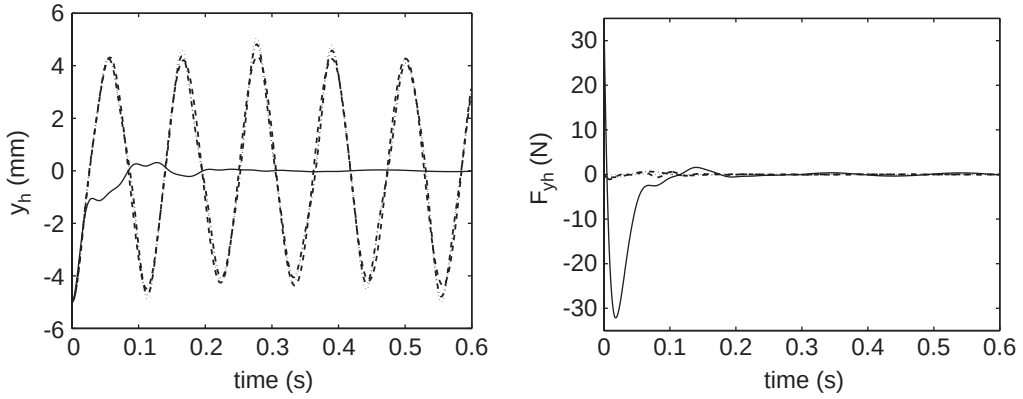

Fig. 9. Hub movement in the y-direction and the control force applied using the three designed control schemes. The non-controlled response ($\cdots$), control by scheme 1 ($-\cdot-$), by scheme 2 ($--$) and by scheme 3 (—).

to separate from each other because in some cases they are coincident. The frequency responses of the controlled system show that just those modes addressed by the controllers are suppressed, whereas the residual modes are still present. The frequency components identified by the frequency responses in Fig. 11 correspond exactly to the mode shapes shown in Figs. 3–5. The presence of parametric vibration modes, at frequencies $\omega \pm \Omega$ Hz, due to the strong coupling among blade and rotor motion, is clearly observed. For example, mode 1 results in a hub movement in x_h at the frequency $\omega = 7.76$ Hz and in two parametric components of blade vibrations at the frequencies $\omega = 7.76 \pm \Omega$ Hz.

5. Conclusion

Application of active control for vibration suppression in coupled rotor–blade systems has been investigated theoretically. A methodology for designing a periodic time-variant modal controller for vibration suppression in this type of system has been presented.

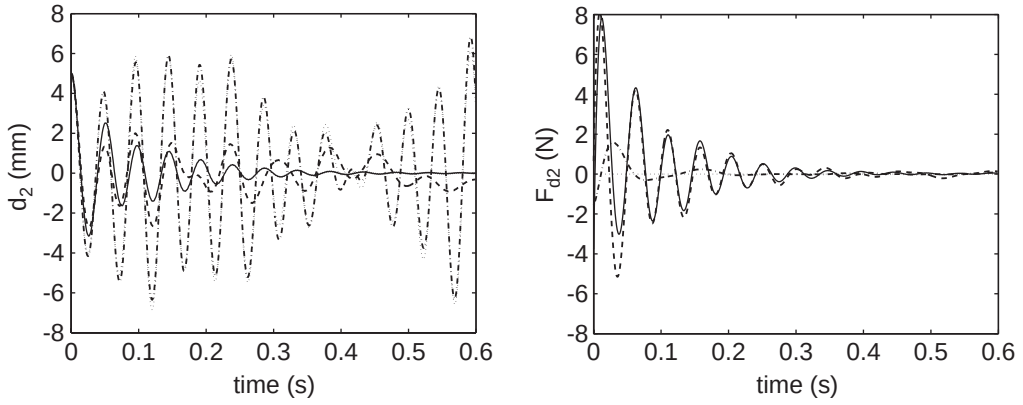

Fig. 10. Tip point deflection of blade 2 and the control force applied to the blade using the three designed control schemes. The non-controlled response (· · ·), control by scheme 1 (– · –), by scheme 2 (––) and by scheme 3 (—).

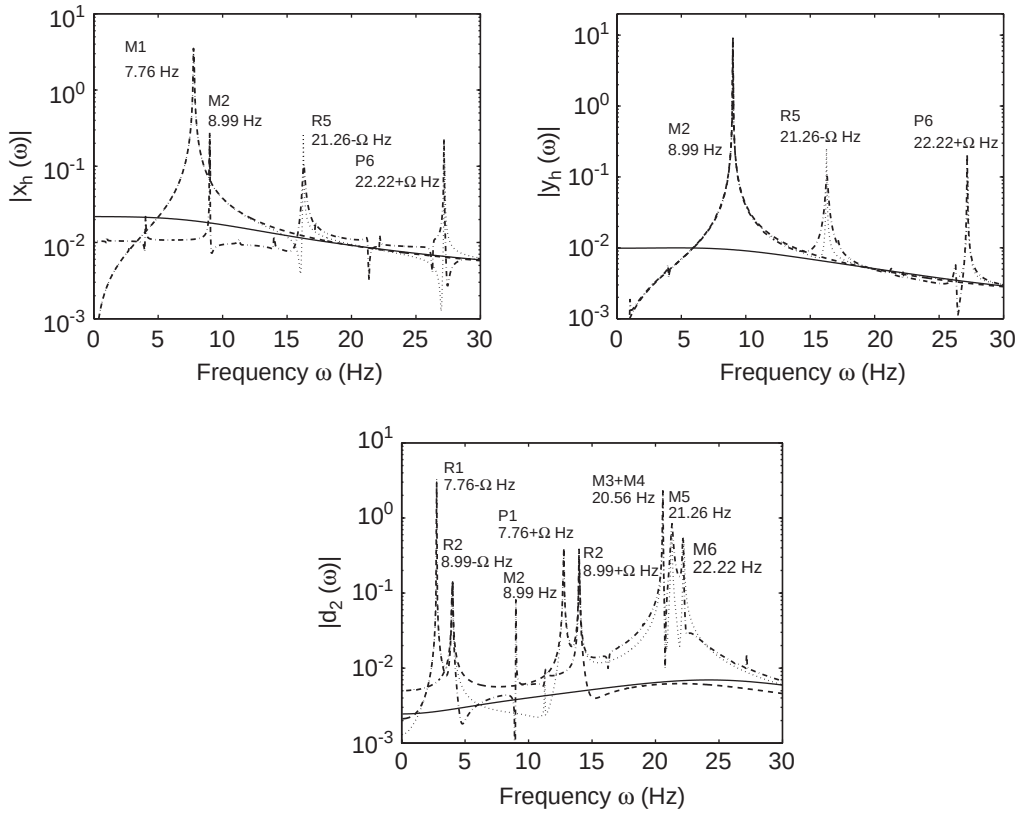

Fig. 11. Frequency spectrum diagrams of the hub lateral movements and blade 2's deflection using the three control schemes. The non-controlled response (· · ·), control by scheme 1 (– · –), by scheme 2 (––) and by scheme 3 (—).

A mathematical model for a coupled rotor–blade system has been established and transformed into a time-invariant modal form using a periodic modal transformation.

Using the transformed model a periodic modal state feedback controller, able to cope with the periodicity, is designed with help of the linear time-invariant LQR-control technique. Furthermore, the modal decoupling of the equations of motion implies that the controller order is easily reduced.

The effectiveness of the designed control methodology is numerically examined using the mathematical model and the numerical investigation shows that the rotor and blade vibrations can be efficiently suppressed. Specific vibration modes, basis modes and their associated parametric forward and backward rotating parts can be separately addressed and suppressed.

Moreover, the controller design methodology presented based on modal analysis in time-variant systems, provides a very effective tool for analysis of the system modal controllability and observability. The mode shapes are visually examined and modal controllability and observability indices are easily calculated. This visual examination and the calculated measures are very useful in order to identify suitable locations for sensors and actuators. For the rotor–blade system under consideration with four identical blades, such analysis shows that actuators and sensors have to be implemented, which act on both the hub and on each blade in order to control and observe all state variables.

Finally, it can be concluded that, when designing active controllers for this special kind of system, the modal transformation based on modal analysis in time-variant systems is very useful: (I) it gives a mathematical explanation of all the frequencies and vibration modes of the system, i.e. basis and parametric modes; (II) it provides the possibility of doing a 'physical' order reduction so that only troublesome modes are controlled; (III) it provides an easy method for the identification of optimal actuator and sensor placement.

References

[1] I.F. Santos, C.M. Saracho, J.T. Smith, J. Eiland, Contribution to experimental validation of linear and non-linear dynamic models for representing rotor–blade parametric vibrations, *Journal of Sound and Vibration* 271 (3–5) (2004) 883–904.

[2] M.J. Balas, Modal control of certain flexible dynamic systems, *SIAM Journal of Control and Optimization* 16 (3) (1978) 450–462.

[3] R. Firoozian, R. Stanway, Active vibration control of turbomachinery: a numerical investigation of modal controllers, *Mechanical Systems and Signal Processing* 2 (3) (1988) 243–264.

[4] J. Kaneko, H. Kano, Modal control of flexible one-link arms with random disturbances, *Proceedings of the 28th IEEE Conference on Decision and Control*, 1989, pp. 2141–2146.

[5] C. Chantalakhana, R. Stanway, Active constrained layer damping of plate vibrations: a numerical and experimental study of modal controllers, *Smart Materials and Structures* 9 (2000) 940–952.

[6] Y.A. Khulief, Vibration suppression in rotating beams using active modal control, *Journal of Sound and Vibration* 242 (4) (2001) 681–699.

[7] P.C. Chen, I. Chopra, Induced strain actuation of composite beams and rotor blades with embedded piezoceramic elements, *Smart Materials and Structures* 5 (1996) 35–48.

[8] A. Baz, J. Ro, Vibration control of rotating beams with active constrained layer damping, *Smart Materials and Structures* 10 (2001) 112–120.

[9] P. Arcara, S. Bittanti, M. Lovera, Periodic control of helicopter rotors for attenuation of vibrations in forward flight, *IEEE Transactions on Control Systems Technology* 8 (6) (2000) 883–894.
[10] S. Bittanti, F.A. Cuzzola, Periodic active control of vibrations in helicopters: a gain-scheduled multi-objective approach, *Control Engineering Practice* 10 (2002) 1043–1057.
[11] R.A. Calico, W.E. Wiesel, Control of time-periodic systems, *Journal of Guidance, Control and Dynamics* 7 (6) (1984) 671–676.
[12] A.J. Calise, M.E. Wasikowski, D.P. Schrage, Optimal output feedback for linear time-periodic systems, *Journal of Guidance, Control and Dynamics* 15 (2) (1992) 416–423.
[13] S.C. Sinha, P. Joseph, Control of general dynamic systems with periodically varying parameters via Liapunov–Floquet transformation, *Journal of Dynamic Systems, Measurement and Control* 116 (1994) 650–658.
[14] D.B. Marghitu, S.C. Sinha, C. Diaconescu, Control of a parametrically excited flexible beam undergoing rotation and impacts, *Multibody System Dynamics* 3 (1) (1999) 47–63.
[15] G. Szasz, G.T. Flowers, Time periodic control of a bladed disk assembly using shaft based actuation, *Journal of Vibration and Acoustics* 123 (2001) 395–401.
[16] J. Xu, R. Gasch, Modale Behandlung linearer periodisch zeitvarianter Bewegungsgleichungen, *Archive of Applied Mechanics* 65 (3) (1995) 178–193 (in German).
[17] CM. Saracho, I.F. Santos, Modal analysis in periodic, time-varying systems with emphasis to the coupling between flexible rotating beams and non-rotating flexible structures, *Proceedings of the X International Symposium on Dynamic Problems in Mechanics*, 2003, pp. 399–404.
[18] R.H. Christensen, I.F. Santos, Active control of parametric vibrations in coupled rotor–blade systems, *Proceedings of the Tenth International Congress on Sound and Vibration*, 2003, pp. 323–330.
[19] CM. Saracho, I.F. Santos, Dynamic models for coupled blade–rotor vibrations, *Proceedings of the IX International Symposium on Dynamic Problems in Mechanics*, 2001, pp. 263–268.
[20] F. Reuter, Coupling of elastic and gyroscopic modes of rotating disc structures, *Proceedings of the Fifth International Conference on Rotor Dynamics IFToMM*, 1998, pp. 443–455.
[21] A.M.A. Hamdan, A.H. Nayfeh, Measure of modal controllability and observability for first- and second-order linear systems, *Journal of Guidance, Control and Dynamics* 12 (3) (1989) 421–428.
[22] R.C. Fenn, J.R. Downer, D.A. Bushko, V. Gondhalekar, N.D. Ham, Terfenol driven flaps for helicopter vibration reduction, *Smart Materials and Structures* 5 (1996) 49–57.
[23] M. Zielinski, G. Ziller, Noncontact vibration measurements on compressor rotor blades, *Measurement Science Technology* 11 (2000) 847–856.
[24] B.O. Al-Bedoor, Blade vibration measurement in turbo-machinery: current status, *The Shock and Vibration Digest* 34 (6) (2002) 455–461.
[25] G. Schweitzer, Magnetic bearings as a component of smart rotating machinery, *Proceedings of the Fifth International Conference on Rotor Dynamics*, 1998, pp. 3–15.
[26] H. Ulbrich, Active vibration control of rotors, *Proceedings of the Fifth International Conference on Rotor Dynamics*, 1998, pp. 16–31.
[27] A. Alizadeh, C. Ehmann, U. Schonhoff, R. Nordmann, Active bearing of rotors utilizing robust controlled piezo actuators, *Proceedings of ASME DETC'03* (paper DETC2003/VIB-48850), Chicago, IL, USA, 2003.
[28] I.F. Santos, A. Scalabrin, Control system design for active lubrication with theoretical and experimental examples, *Journal of Engineering for Gas Turbines and Power* 125 (1) (2000) 75–80.
[29] J. Althaus, H. Ulbrich, A fast hydraulic actuator for active vibration control, *Proceedings of the Fifth International Conference on Vibrations in Rotating Machinery*, Bath, England, 1992.
[30] I.F. Santos, Design and evaluation of two types of active tilting pad journal bearings, *Proceedings of IUTAM Symposium on Active Control of Vibration*, Bath, England, 1994, pp. 79–87.
[31] H. Irretier, Mathematical foundations of experimental modal analysis in rotor dynamics, *Mechanical Systems and Signal Processing* 13 (2) (1999) 183–191.